

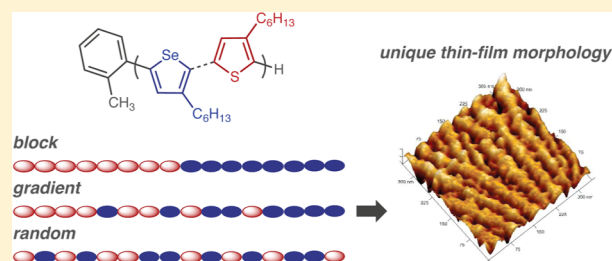
Impact of Copolymer Sequence on Solid-State Properties for Random, Gradient and Block Copolymers containing Thiophene and Selenophene

Edmund F. Palermo and Anne J. McNeil*

Department of Chemistry and Macromolecular Science and Engineering Program, University of Michigan, 930 North University Avenue, Ann Arbor, Michigan 48109-1055, United States

S Supporting Information

ABSTRACT: Nickel-catalyzed chain-growth copolymerizations of thiophene and selenophene derivatives afforded well-defined π -conjugated copolymers with narrow molecular weight distributions, defined end-groups, and specific sequences. In particular, a π -conjugated copolymer with a novel linear gradient sequence was prepared. Compared to the analogous block and random copolymers, the gradient copolymer displayed unique optical and thermal properties as well as thin-film morphology. Moreover, the gradient copolymer exhibited an intermediate extent of phase separation into thiophene-rich and selenophene-rich domains compared to the block and random copolymers. Because this gradient sequence provides access to new solid-state properties, these materials should be further explored in applications where phase-separated morphology is important (e.g., solar cells, transistors, and light-emitting diodes).



INTRODUCTION

Organic π -conjugated polymers are crucial components in a broad range of practical applications, including organic photovoltaic devices,¹ chemical and biological sensors,² and biomedical implants.³ Most conjugated polymers are synthesized by transition metal-catalyzed cross-coupling reactions, such as Stille,⁴ Sonogashira,⁵ and Suzuki⁶ reactions, which have traditionally been considered step-growth processes. Although these methods have afforded useful materials, the random coupling reactions inherent in step-growth procedures limits control over copolymer sequence. In 2004, Yokozawa⁷ and McCullough⁸ independently discovered a Ni-catalyzed polymerization that proceeds by a chain-growth mechanism through a putative Ni(0)–polymer π -complex.^{9–11} This synthetic method has yielded polythiophenes with well-defined molecular weights, high regioregularities, low polydispersities and control over end-group functionalization.¹² This chain-growth method also enables unprecedented control over the copolymer's sequence distribution.¹³ For example, gradient copolymers, in which the composition varies gradually along the polymer chain, can now be prepared.¹⁴

Gradient copolymers are interesting targets because those made from vinyl monomers have exhibited unique physical and morphological properties relative to the analogous block and random copolymers.¹⁵ Gradient copolymers with a π -conjugated backbone have been difficult to access because there are a limited number of monomers that undergo chain-growth copolymerization.¹⁶ Despite this challenge, we recently synthesized the first example of a gradient π -conjugated copolymer using two thiophene monomers containing either

a hexyl or hexyloxymethyl side chain.¹⁴ Many of the resulting copolymer properties were similar to the homopolymers because of the similarities in monomer structure.¹⁴ Therefore, the effect of gradient sequence distribution on π -conjugated polymer properties has remained largely unknown. To fill this gap, the synthesis of π -conjugated gradient copolymers composed of chemically dissimilar repeating units is needed. Selenophene derivative (1) and a thiophene derivative (2) were selected for this study because Seferos and co-workers demonstrated that their random and block copolymers could be prepared under chain-growth conditions.¹⁷ Furthermore, poly(3-hexylselenophene) (P3HS) has been extensively characterized¹⁸ and used in photovoltaic devices¹⁹ due to its reduced band gap relative to poly(3-hexylthiophene) (P3HT). Herein, we report the synthesis of gradient, random, and block copolymers composed of selenophene 1 and thiophene 2, all of which exhibited unique solid-state properties. Most significantly, the newly prepared gradient copolymer displayed a thin-film morphology and extent of phase separation that was intermediate between the random and block copolymers. As a consequence, these gradient copolymers could be useful in optoelectronic applications, where phase-separated morphology plays an integral role in device performance.²⁰

Received: June 4, 2012

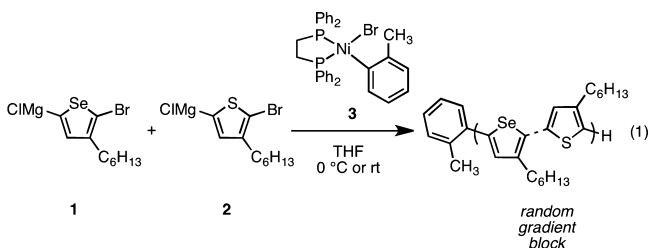
Revised: July 6, 2012

Published: July 20, 2012

RESULTS AND DISCUSSION

To elucidate the effect of copolymer sequence on thin-film properties, random, gradient, and block copolymers were synthesized with similar compositions, number-average molecular weights, molecular weight distributions, and regioregularities.

Copolymer Syntheses. General. An aryl-functionalized nickel catalyst (**3**)²¹ was selected for these copolymerizations to avoid propagation from both ends of the polymer²² and to enable precise control over the polymer sequence. Using this catalyst, both homo- and copolymerizations of 2-bromo-5-magnesiochloride-3-hexylselenophene (**1**) and 2-bromo-5-magnesiochloride-3-hexylthiophene (**2**) were successful at either 0 °C or room temperature under positive N₂ pressure (eq 1). The chain-growth nature of the homo- and



copolymerizations was evident by the linear increases in the number-average molecular weight (M_n) with conversion and further supported by the MALDI-TOF MS analysis of low molecular weight polymers, which exhibited peaks consistent with exclusively tolyl/H end-groups (see Supporting Information).

Batch copolymerizations were used to determine the copolymerization rates of monomers **1** and **2** catalyzed by **3**. Aliquots were drawn periodically and analyzed by GC to determine the conversion of each comonomer as a function of time (Supporting Information). The cumulative mole fraction of **2** in the copolymer was determined based on this conversion data. As evident in Figure 1A, the copolymer M_n increased linearly with overall conversion, while the polydispersity index (PDI) remained low, consistent with a controlled chain-growth polymerization. A series of batch copolymerizations were performed with different initial comonomer feed compositions to determine the reactivity ratios (Supporting Information). These data were fit using the classical Mayo–Lewis equation²³ and a nonlinear least-squares regression, giving reactivity ratios of $r_1 = 1.56 \pm 0.08$ and $r_2 = 0.52 \pm 0.03$ (Figure 1B and Supporting Information). These reactivity ratios are consistent with the observation that selenophene monomer **1** is consumed slightly faster than thiophene monomer **2** (Supporting Information). Because the two monomers are competing during the transmetalation step of the catalytic cycle, the differences in reactivity must occur at this step. The faster rate of transmetalation for **1** can be rationalized based on the fact that selenium is slightly less electronegative than sulfur, which makes the anionic carbon in **1** more nucleophilic than **2**. Despite these small rate differences, the reactivity ratios are both near 1.0 and therefore the batch copolymerizations produced copolymers with largely random sequences and only a slight compositional drift along the polymer chain. For example, the 1:1 batch copolymerization drifts from approximately 60% selenophene at low conversion to a final value of about 50% selenophene (Supporting Information).

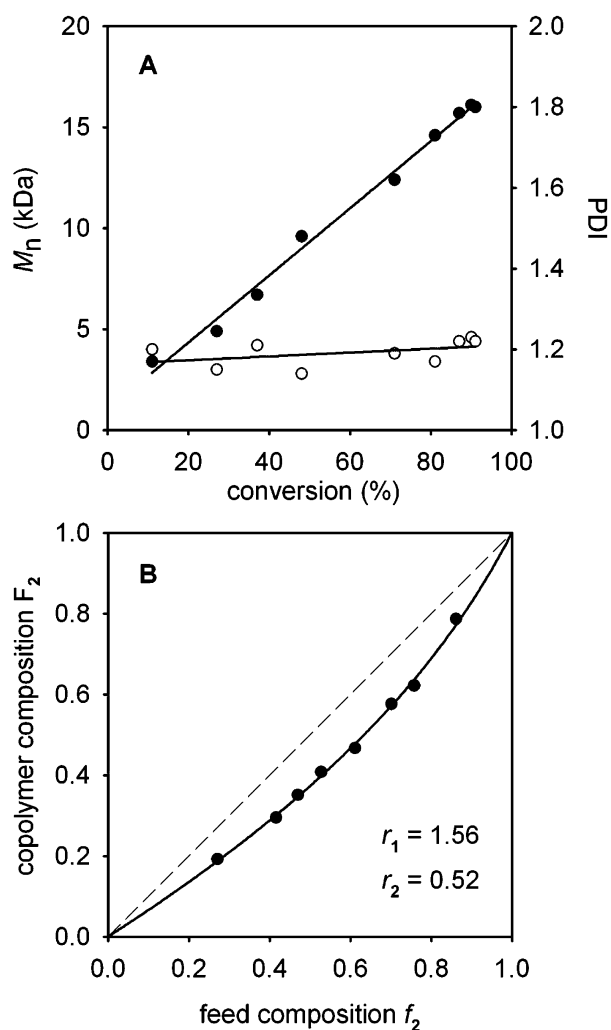


Figure 1. (A) Plot of the number-average molecular weight (M_n , ●) and polydispersity index (PDI, ○) versus % conversion for the batch copolymerization of **1** and **2** (1:1 mol ratio) catalyzed by **3** (1 mol %) at 0 °C in THF. (B) Plot of the thiophene copolymer composition (F_2) versus thiophene feed composition (f_2) for eight different batch copolymerizations. The solid curve represents a nonlinear least-squares fit to the Mayo–Lewis equation (see Supporting Information). The dashed line represents the ideal case where $r_1 = r_2 = 1$.

Gradient Copolymer Synthesis. Linear gradient copolymers were obtained using syringe-pump addition of selenophene monomer **1** to a solution containing thiophene monomer **2** and catalyst **3**. The rate of monomer addition was chosen based on the homopolymerization rate of **2** and then further tuned to account for the differences in their reactivity ratios. This fixed rate of addition produced a copolymer with a linear gradient sequence as evident by the linear increase in the cumulative mole fraction of **1** in the copolymer with an increase in the normalized chain length (Figure 2). Gradient copolymers with a M_n of 10–15 kDa and PDI of about 1.1–1.2 were obtained at 0 °C. Higher molecular weight copolymers were difficult to obtain because of their limited solubility in THF at this temperature.

To prepare higher molecular weight copolymers, the copolymerizations were carried out at room temperature (Supporting Information). A linear gradient copolymer was thus obtained with a M_n of 31.9 kDa and a PDI of 1.13 (Figure 3A and Supporting Information). The ¹H NMR spectrum

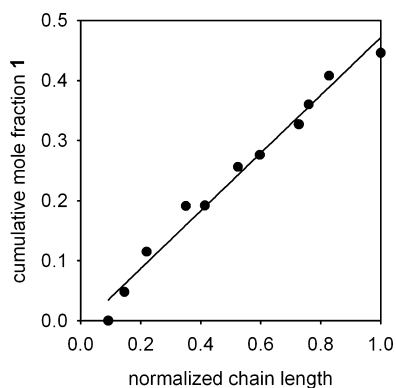


Figure 2. Plot of the cumulative mole fraction of **1** in the copolymer versus the normalized chain length for the gradient copolymerization of **1** and **2** catalyzed by **3** in THF at 0 °C.

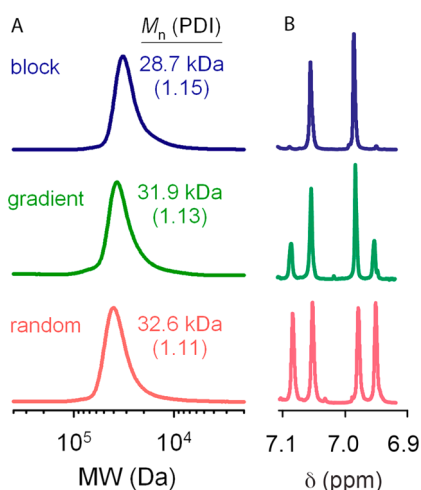


Figure 3. Characterization data for the block, gradient, and random copolymers. (A) GPC data relative to PS standards in THF. (B) Selected region of the ¹H NMR spectra.

revealed that the regioregularity was >98% and the molar composition (1:2) matched the intended ratio of 1:1 (Supporting Information). The high regioregularity suggests that the minor regioisomers of both **1** and **2** are largely unreactive under these conditions. End-group analysis showed a degree of polymerization (DP = 106) similar to the monomer-to-initiator mole ratio of 100:1, which is consistent with a chain-growth polymerization. The gradient sequence distribution is evident based on an analysis of the chemical shifts of the backbone protons (Figure 3B). For example, resonances at 6.98 and 7.12 ppm correspond to segments of the polymer chain enriched in poly(3-hexylthiophene) and poly(3-hexylselenophene), respectively. In addition, resonances at 6.92 and 7.18 ppm are indicative of heterogeneous segments containing thiophene-selenophene and selenophene-thiophene dyads.^{17c} As anticipated, the gradient copolymer exhibited all four resonances with unequal areas. The relative integrations reveal that the sequence distribution consists largely of thiophene and selenophene oligomers surrounding a smaller region of heterogeneous dyads. These data, combined with the linear change in the copolymer composition, are consistent with a gradient sequence copolymer.

Block Copolymer Synthesis. The analogous block copolymer was prepared (with minor modifications to the published

procedure^{17a,c}) to compare the effect of copolymer sequence on polymer properties. The first block was prepared by adding catalyst **3** to monomer **2** and stirring at rt for 1 h. To this macroinitiator block ($M_n = 12.5$ kDa, PDI = 1.09) was added monomer **1** followed by stirring at rt for an additional 1 h. The resulting block copolymer showed a M_n of 28.7 kDa and a PDI of 1.15 by GPC analysis (Figure 3A). The absence of a shoulder peak in the low molecular weight region suggests quantitative block extension without chain termination. The ¹H NMR spectrum of the block copolymer revealed that the mole fraction of **2** in the copolymer was 0.47, the regioregularity was >98%, and the DP was 103 (Supporting Information). As expected from the block sequence distribution and molar composition, there was an almost equal ratio of the resonances corresponding to the two homopolymers (Figure 3B). Combined, these data indicate that the block copolymer has a similar molecular weight, molecular weight distribution, regioregularity and molar composition to the gradient copolymer.

Random Copolymer Synthesis. The random copolymer was prepared for comparison to the block and gradient copolymers. The random copolymer was prepared by batch copolymerization of **1** and **2** using catalyst **3** at rt in THF (Supporting Information). GPC analysis revealed a M_n of 32.6 kDa and a PDI of 1.11 (Figure 3A). The ¹H NMR spectrum showed that the mole fraction of **2** was 0.51, the regioregularity was >98%, and the DP was 112 (Supporting Information). As anticipated, based on the sequence distribution and molar composition, the random copolymer exhibited all four resonances with similar areas, indicating that the distribution of homogeneous and heterogeneous dyads was random (Figure 3B).

To summarize, each of the synthesized copolymers exhibit similar molecular weights, PDIs, regioregularities and molar compositions (~1:1). Because the only difference is their sequence distribution, these materials can be used to elucidate the effect of copolymer sequence on the solid-state physical and optical properties of π -conjugated copolymers.

Copolymer Characterization. Optical Properties. In dilute CHCl₃ solutions, each of the copolymers exhibited a broad absorption profile with a peak maximum near 467–470 nm, which is intermediate between that of P3HT ($\lambda_{max} = 450$ nm) and P3HS ($\lambda_{max} = 490$ nm). The similar absorption spectra for all three copolymers in solution, despite their different sequences, suggest that short oligomers are the chromophores due to a nonplanar conformation along the copolymer backbone.

Thin films were prepared by spin-casting from chlorobenzene solutions onto glass substrates. The as-cast films exhibited red shifts typical of semicrystalline conjugated polymers, reflecting the increased planarization of the polymer backbone and larger effective conjugation length in the solid-state (Supporting Information). After isothermal recrystallization in a vacuum oven,²⁴ an increased degree of interchain aggregation was evident.²⁵ For example, the block copolymer absorbance spectrum featured prominent peaks corresponding to the weakly coupled H-aggregates of pure P3HS^{18a} and pure P3HT²⁵ (685 and 610 nm, Figure 4), which suggests that the block copolymer is phase separating into **1**-rich and **2**-rich domains. The gradient copolymer also exhibited similar aggregate-based peaks (670 and 605 nm), though less prominent, suggesting an intermediate extent of domain separation in the solid state. In contrast, the random copolymer showed a single, weak absorption peak in that region, which

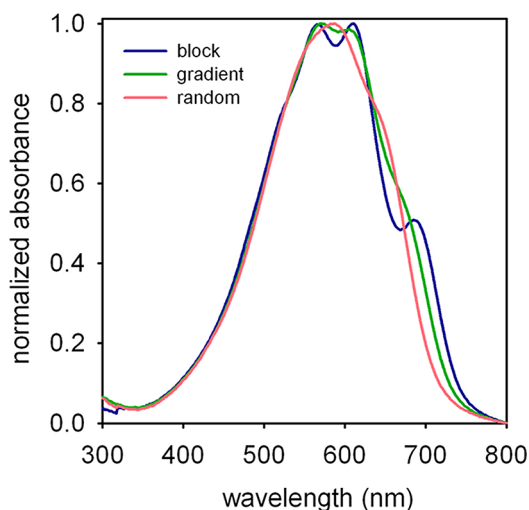


Figure 4. UV-vis absorbance spectra of thin films of the block, gradient, and random copolymers after isothermal recrystallization.

indicates a more homogeneous composition. Overall, these results demonstrate that the photophysical properties of π -conjugated copolymers in the solid-state are sequence-dependent, and may result from differences in their extent of phase separation (vide infra).

Thermal Properties. The copolymers were analyzed by differential scanning calorimetry (DSC) to probe their crystallinity. No identifiable glass transitions were observed for any of the copolymers. Instead, each copolymer exhibited a sharp melting endotherm and a corresponding crystallization exotherm (Supporting Information). These results are expected for semicrystalline polymers and are consistent with their high regioregularities²⁶ and low polydispersities.²⁷ To obtain the most stable morphology, DSC thermograms were also acquired after isothermal recrystallization at 220 °C for 1 h (Supporting Information).²⁴ As evident in Figure 5, the peak temperature of the melting endotherms exhibited a dependence on the copolymer sequence. Specifically, the block copolymer melted at a higher temperature ($T_m = 242$ °C) than the gradient copolymer ($T_m = 238$ °C) and the random copolymer ($T_m =$

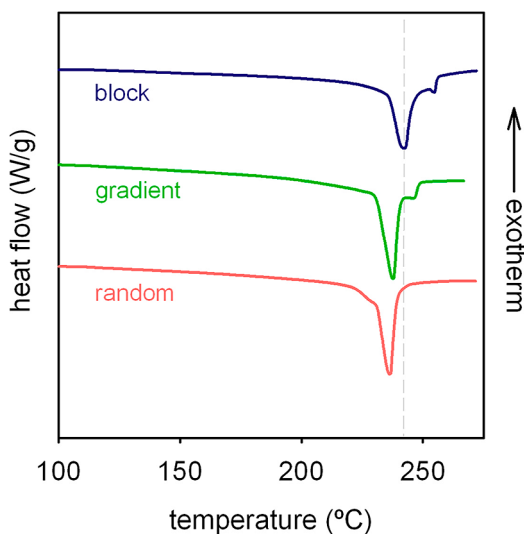


Figure 5. Differential scanning calorimetry data for the block, gradient, and random copolymers.

236 °C). The increased melting temperature for the block copolymer implies that the solid-state packing is more stable than the gradient and random copolymers, which could indicate a more phase-separated morphology if the interchain interactions between thiophene–thiophene and selenophene–selenophene are more stable than the thiophene–selenophene interactions. Interestingly, all copolymer melting temperatures are lower than the homopolymers (P3HT (243 °C) and P3HS (256 °C) with similar M_n and PDI, see Supporting Information), which suggests that the cocrystallization of segments containing these two different repeating units are destabilized relative to the pristine crystallites. A shoulder peak on the high temperature side is observed in the melting endotherms of the block and gradient copolymers, which is indicative of spontaneous reorganization/recrystallization of the melting polymer chains into more ordered structures.²⁸ The absence of such a feature in the case of the random copolymer suggests a reduced degree of solid-state organization. Combined with the absorbance data, these results indicate that the solid-state packing interactions between the polymer chains depend on the copolymer sequence distribution and suggest that phase separation may be occurring.

Thin-Film Morphologies. Atomic force microscopy (AFM) was performed on thin films of each copolymer after isothermal recrystallization (Supporting Information and Figure 6).²⁴ The phase data is presented herein because it has been shown to provide higher contrast images than the height data with π -conjugated block copolymers.²⁹ As evident in Figure 6A, the block copolymer organized into densely packed lamellar domains with sharp interfaces between regions of high and low phase contrast after isothermal recrystallization. These features ranged from 30 to 40 nm in thickness, which correspond to the theoretical end-to-end distance for a fully extended chain with DP of 100 (38–39 nm), suggesting that these nanofibers result from crystallization of extended chains and are presumably driven by strong interchain interactions.^{30,31} The high contrast regions likely correspond to the crystalline domains, with the extended polymer chains arranged perpendicular to the nanofiber axis, whereas the low contrast regions correspond to amorphous segments near the chain ends.²⁹ Seferos and co-workers reported AFM phase images of a similar block copolymer that exhibited either worm-like or nanowire morphologies, depending on the conditions.¹⁷ Hence, it is important to emphasize that processing conditions are crucial factors in generating any thin-film morphology. As a consequence, we used identical spin-casting and recrystallization conditions to compare the block, gradient, and random copolymers and determine the impact of copolymer sequence on thin-film morphology (Supporting Information).

The AFM image of the gradient copolymer films also revealed lamellar domains after isothermal recrystallization.³² However, the interfaces between high and low contrast regions are less sharply defined, implying a more gradual interface between the crystalline and amorphous domains (Figure 6B). This result suggests that the gradient sequence distribution diminishes the interchain interactions that lead to the lamellar domains. In contrast, the AFM image of the random copolymer displayed an entirely different morphology characterized by the coexistence of high aspect ratio nanofibers dispersed in a matrix of small, disorganized crystallites. This morphology reflects a further reduction in the interchain interactions due to the random sequence of comonomers throughout the chain. The 2D fast Fourier transform (FFT) of the AFM images revealed

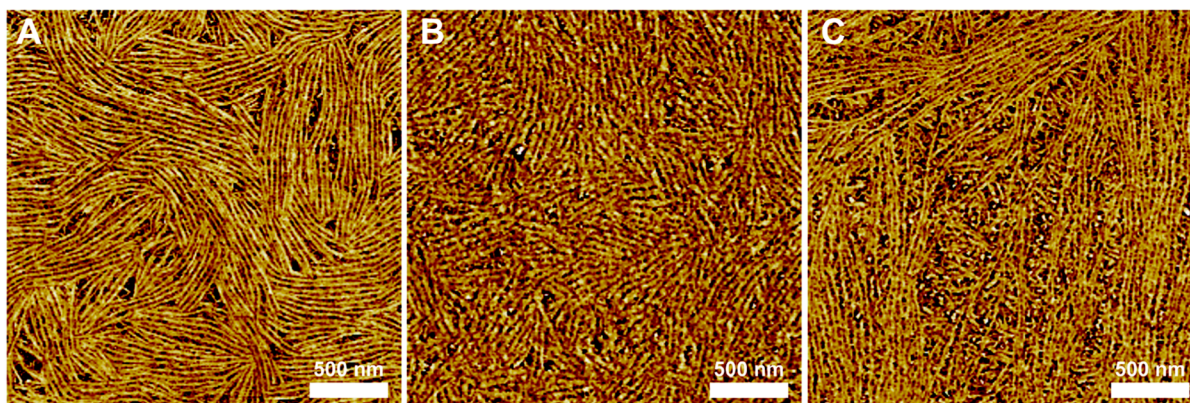


Figure 6. Tapping mode atomic force microscopy (AFM) phase images of (A) block, (B) gradient, and (C) random copolymer thin films after isothermal recrystallization. (Higher resolution images can be found in the Supporting Information.)

that the periodicity of phase contrast was greatest for the block, followed by the gradient and random copolymers, suggesting that the more segregated sequence distribution enhances the organization of the lamellae (Supporting Information). Overall, these results indicate that the copolymer sequence leads to unique nanoscale morphologies.

Because the AFM images cannot be used to distinguish between thiophene-rich and selenophene-rich regions, small-angle X-ray scattering (SAXS) data was acquired.³³ SAXS is a well-suited tool for studying periodic fluctuations of electron density on the order of 10–100 nm in phase-separated polymer systems. On the basis of the morphologies observed by AFM and the extent of interchain interactions observed in the UV–vis absorption spectra, we anticipated that the block copolymer would exhibit the greatest extent of periodic organization, followed by the gradient and random copolymers. Indeed, the block copolymer showed the most significant amount of X-ray scattering compared to the gradient and random copolymers (Supporting Information). In the Lorentz-corrected spectra, which eliminates the effects of the experimental geometry and isolates the Bragg reflections, the block and gradient copolymers exhibited a peak at nearly the same scattering vector (q), suggesting that both materials possess periodic arrangements of electron-dense regions with spacing on the order of 30 nm (Figure 7). In contrast, the random copolymer showed no discernible peak. The integrated area under the

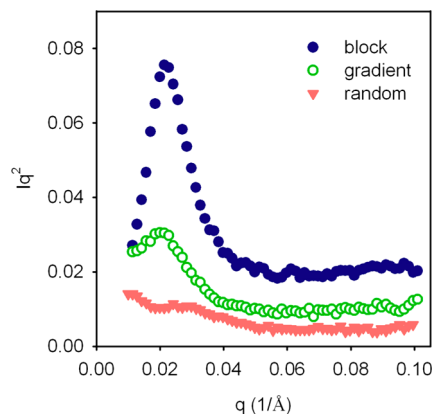


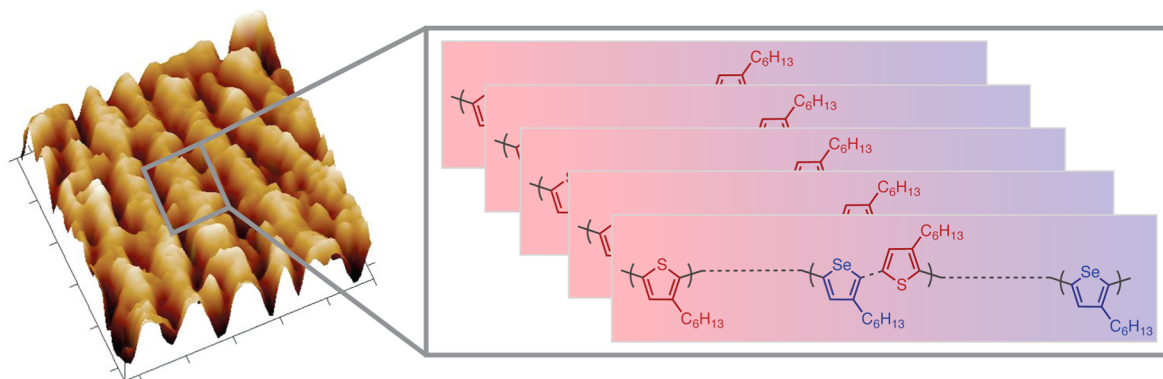
Figure 7. Plot of the Lorentz-corrected intensity (Iq^2) versus scattering vector (q) for the copolymers after isothermal recrystallization.

curve is known as the invariant Q , which represents the extent of phase separation.³³ On the basis of the integrated areas, the gradient copolymer exhibits less pronounced phase separation than the block copolymer but significantly more phase separation than the random copolymer. In addition, the scattering profile observed for the block copolymer mirrors the FFT of the AFM image, suggesting similar lamellar morphologies in the bulk sample and the thin film. Overall, these results indicate that the copolymer sequence can be used to influence the extent of phase separation.

SUMMARY

The consistent picture that emerges from these studies is that copolymer sequence dramatically influences the solid-state organization of semicrystalline materials. Most significantly, the newly synthesized and characterized gradient copolymer exhibited an extent of phase separation and domain segregation that is intermediate between that of the block and random copolymers. These conclusions are based on: (1) The relative magnitudes of the aggregate-based peaks in the absorption spectra, which revealed that the extent of thiophene–thiophene and selenophene–selenophene aggregates was greatest in the block copolymer, followed by the gradient copolymer and then random copolymer. (2) The relative ordering of melting temperatures, which suggested that the interchain interactions were strongest in the block copolymer, followed by the gradient copolymer and then random copolymer. (3) The extent and nature of lamellar formation, which was greatest in the block copolymer, followed by the gradient copolymer and weakest in the random copolymer. (4) The intensity of scattered X-rays, which revealed that the lamellar organization is most significant in the block copolymer, followed by the gradient copolymer and not at all significant in the random copolymer. From these data, we suggest that the solid-state organization of the gradient copolymers involves alignment of the block-like regions at the chain termini with overlapping midsections consisting of a gradual transition between the two monomers (Scheme 1). Note that although this lamellar-type morphology is qualitatively similar to that observed for the block copolymer, the internal structure of these aggregates, and their resulting thermal and optical properties, are measurably different. Thus, gradient π -conjugated copolymers can provide access to new morphologies for various optoelectronic applications.

Scheme 1. Proposed Organization of the Gradient Copolymers within the Nanofibers



CONCLUSIONS

Copolymers of thiophene and selenophene derivatives with random, block, and linear gradient sequences were prepared in a controlled fashion using a Ni-catalyzed chain-growth polycondensation. Tuning the copolymer sequence led to subtle changes in the solid-state thermal and optical properties, while dramatically affecting the thin-film morphology and extent of phase separation. In each case, the properties of the gradient copolymer were intermediate between those of the random and block analogues. Because morphology is an important factor in optoelectronic applications,²⁰ these new materials may well lead to improved device performance. It is important to note, however, that the processing conditions will greatly impact the active layer morphology, and the phase diagram will be further complicated when these materials are blended with others (e.g., fullerenes). These studies represent an interesting avenue for future work.

ASSOCIATED CONTENT

Supporting Information

Experimental details and spectroscopic data. This material is available free of charge via the Internet at <http://pubs.acs.org>.

AUTHOR INFORMATION

Corresponding Author

*E-mail: ajmcneil@umich.edu

Notes

The authors declare no competing financial interest.

ACKNOWLEDGMENTS

We thank the National Science Foundation (CAREER CHE-0954610) for support of this work. We also thank Mr. Weiwei Wu and Mr. Harry L. van der Laan for assisting with characterization data. A.J.M. thanks the Alfred P. Sloan Foundation for a research fellowship.

REFERENCES

- (1) For recent reviews, see: (a) Li, G.; Zhu, R.; Yang, Y. *Nature Photon.* **2012**, *6*, 153–161. (b) Boudreault, P.-L. T.; Najari, A.; Leclerc, M. *Chem. Mater.* **2011**, *23*, 456–469. (c) Facchetti, A. *Chem. Mater.* **2011**, *23*, 733–758. (d) Beaujuge, P. M.; Fréchet, J. M. J. *J. Am. Chem. Soc.* **2011**, *133*, 20009–20029. (e) Brabec, C. J.; Gowrisanker, S.; Halls, J. J. M.; Laird, D.; Jia, S. J.; Williams, S. P. *Adv. Mater.* **2010**, *22*, 3839–3856.
- (2) For recent reviews, see: (a) Kim, H. N.; Guo, Z.; Zhu, W.; Yoon, J.; Tian, H. *Chem. Soc. Rev.* **2011**, *40*, 79–93. (b) Lee, K.; Povlich, L.

K.; Kim, J. *Analyst* **2010**, *135*, 2179–2189. (c) Thomas, S. W.; Joly, G. D.; Swager, T. M. *Chem. Rev.* **2007**, *107*, 1339–1386.

(3) For recent reviews, see: (a) Bendrea, A.-D.; Cianga, L.; Cianga, I. *J. Biomater. Appl.* **2011**, *26*, 3–84. (b) Ravichandran, R.; Sundarajan, S.; Venugopal, J. R.; Mukherjee, S.; Ramakrishna, S. *J. R. Soc. Interface* **2010**, *7*, S559–S579. (c) Asplund, M.; Nyberg, T.; Inganäs, O. *Polym. Chem.* **2010**, *1*, 1374–1391.

(4) For a recent review, see: Carsten, B.; He, F.; Son, H. J.; Xu, T.; Yu, L. *Chem. Rev.* **2011**, *111*, 1493–1528.

(5) For a recent review, see: Bunz, U. H. F. *Macromol. Rapid Commun.* **2009**, *30*, 772–805.

(6) For recent reviews, see: (a) Sakamoto, J.; Rehahn, M.; Wegner, G.; Schlüter, A. D. *Macromol. Rapid Commun.* **2009**, *30*, 653–687. (b) Schlüter, A. D. *J. Polym. Sci., Part A: Polym. Chem.* **2001**, *39*, 1533–1556.

(7) (a) Yokoyama, A.; Miyakoshi, R.; Yokozawa, T. *Macromolecules* **2004**, *37*, 1169–1171. (b) Miyakoshi, R.; Yokoyama, A.; Yokozawa, T. *Macromol. Rapid Commun.* **2004**, *25*, 1663–1666.

(8) Sheina, E. E.; Liu, J. S.; Iovu, M. C.; Laird, D. W.; McCullough, R. D. *Macromolecules* **2004**, *37*, 3526–3528.

(9) Though direct evidence of an intermediate π -complex has not yet been obtained, a number of mechanistic studies have been performed. (a) Lee, S. R.; Bryan, Z. J.; Wagner, A. M.; McNeil, A. J. *Chem. Sci.* **2012**, *3*, 1562–1566. (b) Lanni, E. L.; Locke, J. R.; Gleave, C. M.; McNeil, A. J. *Macromolecules* **2011**, *44*, 5136–5145. (c) Lamps, J.-P.; Catala, J.-M. *Macromolecules* **2011**, *44*, 7962–7968. (d) Lanni, E. L.; McNeil, A. J. *Macromolecules* **2010**, *43*, 8039–8044. (e) Tkachov, R.; Senkovskyy, V.; Komber, H.; Sommer, J.-U.; Kiriya, A. *J. Am. Chem. Soc.* **2010**, *132*, 7803–7810. (f) Lanni, E. L.; McNeil, A. J. *J. Am. Chem. Soc.* **2009**, *131*, 16573–16579. (g) Achord, B. C.; Rawlins, J. W. *Macromolecules* **2009**, *42*, 8634–8639. (h) Beryozkina, T.; Senkovskyy, V.; Kaul, E.; Kiriya, A. *Macromolecules* **2008**, *41*, 7817–7823. (i) Miyakoshi, R.; Yokoyama, A.; Yokozawa, T. *J. Am. Chem. Soc.* **2005**, *127*, 17542–17547. (j) Iovu, M. C.; Sheina, E. E.; Gil, R. R.; McCullough, R. D. *Macromolecules* **2005**, *38*, 8649–8656. For recent reviews, see: (k) McNeil, A. J.; Lanni, E. L. *New Conjugated Polymers and Synthetic Methods*. In *Synthesis of Polymers*; Schlüter, D. A., Hawker, C. J., Sakamoto, J., Eds; Wiley-VCH: Germany, 2012; Vol. 1, pp 475–486. (l) Kiriya, A.; Senkovskyy, V.; Sommer, M. *Macromol. Rapid Commun.* **2011**, *32*, 1503–1517.

(10) Ni(0)-arene π -complexes have also been implicated as intermediates in small molecule oxidative addition reactions. For a recent example, see: Li, T.; García, J. J.; Brennessel, W. W.; Jones, W. D. *Organometallics* **2010**, *29*, 2430–2445.

(11) Several Pd catalysts have also exhibited chain-growth polymerization behavior. For recent examples, see: (a) Bryan, Z. J.; Smith, M. L.; McNeil, A. J. *Macromol. Rapid Commun.* **2012**, *33*, 842–847. (b) Verswyvel, M.; Verstappen, P.; De Cremer, L.; Verbiest, T.; Koeckelberghs, G. *J. Polym. Sci., Part A: Polym. Chem.* **2011**, *49*, 5339–5349. (c) Yokozawa, T.; Suzuki, R.; Nojima, M.; Ohta, Y.; Yokoyama, A. *Macromol. Rapid Commun.* **2011**, *32*, 801–806. (d) Elmalem, E.; Kiriya, A.; Huck, W. T. S. *Macromolecules* **2011**, *44*, 9057–9061.

(e) Yokozawa, T.; Kohno, H.; Ohta, Y.; Yokoyama, A. *Macromolecules* **2010**, *43*, 7095–7100. (f) Grisorio, R.; Suranna, G. P.; Mastroianni, P. *Chem.—Eur. J.* **2010**, *16*, 8054–8061. (g) Huang, W.; Su, L.; Bo, Z. *J. Am. Chem. Soc.* **2009**, *131*, 10348–10349. (h) Beryozkina, T.; Boyko, K.; Khanduyeva, N.; Senkovskyy, V.; Horecha, M.; Oertel, U.; Simon, F.; Stamm, M.; Kiriy, A. *Angew. Chem., Int. Ed.* **2009**, *48*, 2695–2698. (i) Yokoyama, A.; Suzuki, H.; Kubota, Y.; Ohuchi, K.; Higashimura, H.; Yokozawa, T. *J. Am. Chem. Soc.* **2007**, *129*, 7236–7237.

(12) For recent examples of polythiophenes prepared via this method, see: (a) Mougner, S.-J.; Brochon, C.; Cloutet, E.; Fleury, G.; Cramail, H.; Hadziioannou, G. *Macromol. Rapid Commun.* **2012**, *33*, 703–709. (b) Yuan, M.; Okamoto, K.; Bronstein, H. A.; Luscombe, C. K. *ACS Macro Lett.* **2012**, *1*, 392–395. (c) Higashihara, T.; Goto, E.; Ueda, M. *ACS Macro Lett.* **2012**, *1*, 167–170.

(13) For recent examples of block, random, and alternating copolymers prepared via this method, see: (a) Lobez, J. M.; Andrew, T. L.; Bulović, V.; Swager, T. M. *ACS Nano* **2012**, *6*, 3044–3056. (b) Wu, Z.-Q.; Radcliffe, J. D.; Ono, R. J.; Chen, Z.; Li, Z.; Bielawski, C. W. *Polym. Chem.* **2012**, *3*, 874–881. (c) Ono, R. J.; Kang, S.; Bielawski, C. W. *Macromolecules* **2012**, *45*, 2321–2326. (d) Miozzo, L.; Battaglini, N.; Braga, D.; Kergoat, L.; Suspène, C.; Yassar, A. *J. Polym. Sci., Part A: Polym. Chem.* **2012**, *50*, 534–541. (e) Verswyvel, M.; Monnaie, F.; Koeckelberghs, G. *Macromolecules* **2011**, *44*, 9489–9498. (f) Kim, J.; Siva, A.; Song, I. Y.; Park, T. *Polymer* **2011**, *52*, 3704–3709. (g) Ohshimizu, K.; Takahashi, A.; Higashihara, T.; Ueda, M. *J. Polym. Sci., Part A: Polym. Chem.* **2011**, *49*, 2709–2714.

(14) Locke, J. R.; McNeil, A. J. *Macromolecules* **2010**, *43*, 8709–8710.

(15) For recent examples, see: (a) Mok, M. M.; Torkelson, J. M. *J. Polym. Sci., Part B: Polym. Phys.* **2012**, *50*, 189–197. (b) Mok, M. M.; Ellison, C. J.; Torkelson, J. M. *Macromolecules* **2011**, *44*, 6220–6226. (c) Mok, M. M.; Masser, K. A.; Runt, J.; Torkelson, J. M. *Macromolecules* **2010**, *43*, 5740–5748. (d) Mok, M. M.; Kim, J.; Wong, C. L. H.; Marrou, S. R.; Woo, D. J.; Dettmer, C. M.; Nguyen, S. T.; Ellison, C. J.; Shull, K. R.; Torkelson, J. M. *Macromolecules* **2009**, *42*, 7863–7876.

(16) (a) Javier, A. E.; Varshney, S. R.; McCullough, R. D. *Macromolecules* **2010**, *43*, 3233–3237. (b) Wu, S.; Bu, L.; Huang, L.; Yu, X.; Han, Y.; Geng, Y.; Wang, F. *Polymer* **2009**, *50*, 6245–6251. (c) Yokoyama, A.; Kato, A.; Miyakoshi, R.; Yokozawa, T. *Macromolecules* **2008**, *41*, 7271–7273. (d) Miyakoshi, R.; Yokoyama, A.; Yokozawa, T. *Chem. Lett.* **2008**, *37*, 1022–1023.

(17) (a) Hollinger, J.; DiCarmine, P. M.; Karl, D.; Seferos, D. S. *Macromolecules* **2012**, *45*, 3772–3778. (b) Li, L.; Hollinger, J.; Coombs, N.; Petrov, S.; Seferos, D. S. *Angew. Chem., Int. Ed.* **2011**, *50*, 8148–8152. (c) Hollinger, J.; Jahnke, A. A.; Coombs, N.; Seferos, D. S. *J. Am. Chem. Soc.* **2010**, *132*, 8546–8547.

(18) (a) Li, L. S.; Hollinger, J.; Jahnke, A. A.; Petrov, S.; Seferos, D. S. *Chem. Sci.* **2011**, *2*, 2306–2310. (b) Heeney, M.; Zhang, W.; Crouch, D. J.; Chabiny, M. L.; Gordyev, S.; Hamilton, R.; Higgins, S. J.; McCulloch, I.; Skabara, P. J.; Sparrowe, D.; Tierney, S. *Chem. Commun.* **2007**, *47*, 5061–5063. (c) For a recent review, see: Patra, A.; Bendikov, M. *J. Mater. Chem.* **2010**, *20*, 422–433.

(19) (a) Klein, M. F. G.; Pfaff, M.; Müller, E.; Czolk, J.; Reinhard, M.; Valouch, S.; Lemmer, U.; Colmann, A.; Gerthsen, D. *J. Polym. Sci., Part B: Polym. Phys.* **2012**, *50*, 198–206. (b) Ballantyne, A. M.; Ferenczi, T. A. M.; Campoy-Quiles, M.; Clarke, T. M.; Maurano, A.; Wong, K. H.; Zhang, W.; Stingelin-Stutzmann, N.; Kim, J.-S.; Bradley, D. D. C.; Durrant, J. R.; McCulloch, I.; Heeney, M.; Nelson, J.; Tierney, S.; Duffy, W.; Mueller, C.; Smith, P. *Macromolecules* **2010**, *43*, 1169–1174. (c) Maurano, A.; Shuttle, C. G.; Hamilton, R.; Ballantyne, A. M.; Nelson, J.; Zhang, W.; Heeney, M.; Durrant, J. R. *J. Phys. Chem. C* **2011**, *115*, 5947–5957. (d) Ballantyne, A. M.; Chen, L. C.; Nelson, J.; Bradley, D. D. C.; Astuti, Y.; Maurano, A.; Shuttle, C. G.; Durrant, J. R.; Heeney, M.; Duffy, W.; McCulloch, I. *Adv. Mater.* **2007**, *19*, 4544–4545.

(20) For recent reviews, see: (a) Chen, W.; Nikiforov, M. P.; Darling, S. B. *Energy Environ. Sci.* **2012**, DOI: 10.1039/c2ee22056c. (b) McNeill, C. R. *Energy Environ. Sci.* **2012**, *5*, 5653–5667. (c) Pivrikas, A.; Neugebauer, H.; Sariciftci, N. S. *Solar Energy* **2011**, *85*, 1226–1237.

(d) Brabec, C. J.; Heeney, M.; McCulloch, I.; Nelson, J. *Chem. Soc. Rev.* **2011**, *40*, 1185–1199. (e) Ruderer, M. A.; Müller-Buschbaum, P. *Soft Matter* **2011**, *7*, 5482–5493. (f) Groves, C.; Reid, O. G.; Ginger, D. S. *Acc. Chem. Res.* **2010**, *43*, 612–620.

(21) Related complexes have been used in Ni-catalyzed polymerizations to generate end-labeled and surface-grafted conjugated polymers. For recent examples, see: (a) Senkovskyy, V.; Senkovska, I.; Kiriy, A. *ACS Macro Lett.* **2012**, *1*, 494–498. (b) Yuan, M.; Okamoto, K.; Bronstein, H. A.; Luscombe, C. K. *ACS Macro Lett.* **2012**, *1*, 392–395. (c) Marshall, N.; Sontag, S. K.; Locklin, J. *Chem. Commun.* **2011**, *47*, 5681–5689. (d) Sontag, S. K.; Sheppard, G. R.; Usselman, N. M.; Marshall, N.; Locklin, J. *Langmuir* **2011**, *27*, 12033–12041. (e) Doubina, N.; Paniagua, S. A.; Soldatova, A. V.; Jen, A. K. Y.; Marder, S. R.; Luscombe, C. K. *Macromolecules* **2011**, *44*, 512–520. (f) Smeets, A.; Willot, P.; De Winter, J.; Gerbaux, P.; Verbiest, T.; Koeckelberghs, G. *Macromolecules* **2011**, *44*, 6017–6025. (g) See also: ref 9a.

(22) Propagation at both ends of the polymer has been attributed to ring-walking of the Ni catalyst during polymerization. For references, see: (a) Komber, H.; Senkovskyy, V.; Tkachov, R.; Johnson, K.; Kiriy, A.; Huck, W. T. S.; Sommer, M. *Macromolecules* **2011**, *44*, 9164–9172. (b) Tkachov, R.; Senkovskyy, V.; Komber, H.; Sommer, J. U.; Kiriy, A. *J. Am. Chem. Soc.* **2010**, *132*, 7803–7810.

(23) Odian, G. *Principles of Polymerization*, 4th ed.; John Wiley & Sons: Hoboken, NJ, 2004; pp 466–469.

(24) This temperature was selected based on the crystallization exotherms observed in the DSC nonisothermal scan. For each of the copolymers, 220 °C is slightly higher than the nonisothermal recrystallization temperature but still below the melting temperature. Hence, recrystallization at this temperature is expected to give the highest accessible degree of crystallite perfection.

(25) (a) Clark, J.; Chang, J.-F.; Spano, F. C.; Friend, R. H.; Silva, C. *Appl. Phys. Lett.* **2009**, *94*, 163306. (b) Gierschner, J.; Huang, Y.-S.; Van Averbeke, B.; Cornil, J.; Friend, R. H.; Beljonne, D. *J. Chem. Phys.* **2009**, *130*, 044105. (c) Clark, J.; Silva, C.; Friend, R. H.; Spano, F. C. *Phys. Rev. Lett.* **2007**, *98*, 206406. (d) Brown, P. J.; Thomas, D. S.; Köhler, A.; Wilson, J. S.; Kim, J.-S.; Ramsdale, C. M.; Sringhaus, H.; Friend, R. H. *Phys. Rev. B* **2003**, *67*, 064203. (e) Spano, F. C. *Acc. Chem. Res.* **2010**, *43*, 429–439.

(26) (a) Snyder, C. R.; Henry, J. S.; DeLongchamp, D. M. *Macromolecules* **2011**, *44*, 7088–7091. (b) Woo, C. H.; Thompson, B. C.; Kim, B. J.; Toney, M. F.; Fréchet, J. M. J. *J. Am. Chem. Soc.* **2008**, *130*, 16324–16329.

(27) Kohn, P.; Huettner, S.; Komber, H.; Senkovskyy, V.; Tkachov, R.; Kiriy, A.; Friend, R. H.; Steiner, U.; Huck, W. T. S.; Sommer, J.-U.; Sommer, M. *J. Am. Chem. Soc.* **2012**, *134*, 4790–4805.

(28) (a) Sommer, J.-U.; Luo, C. *J. Polym. Sci., Part B: Polym. Phys.* **2010**, *48*, 2222–2232. (b) Luo, C.; Sommer, J.-U. *Phys. Rev. Lett.* **2009**, *102*, 147801.

(29) For recent examples, see: (a) Verduzco, R.; Botiz, I.; Pickel, D. L.; Kilbey, S. M.; Hong, K. L.; Dimasi, E.; Darling, S. B. *Macromolecules* **2011**, *44*, 530–539. (b) Zhang, Y.; Tajima, K.; Hashimoto, K. *Macromolecules* **2009**, *42*, 7008–7015.

(30) For related examples, see: (a) Wu, Z.; Petzold, A.; Henze, T.; Thurn-Albrecht, T.; Lohwasser, R. H.; Sommer, M.; Thelakkat, M. *Macromolecules* **2010**, *43*, 4646–4653. (b) Zhang, R.; Li, B.; Iovu, M. C.; Jeffries-EL, M.; Sauvé, G.; Cooper, J.; Jia, S.; Tristram-Nagle, S.; Smilgies, D. M.; Lambeth, D. N.; McCulloch, R. D.; Kowalewski, T. *J. Am. Chem. Soc.* **2006**, *128*, 3480–3481.

(31) Consistent with this hypothesis, AFM images recorded on a copolymer sample with lower molecular weight (gradient sequence, $M_n = 14.4$ kDa, PDI = 1.10) revealed smaller interlamellar spacings (SI).

(32) Lamellar morphologies have been predicted for linear gradient copolymers. For leading references, see: Tito, N. B.; Milner, S. T.; Lipson, J. E. G. *Macromolecules* **2010**, *43*, 10612–10620.

(33) For a recent example of conjugated polymer films analyzed by SAXS, see: Parnell, A. J.; Cadby, A. J.; Mykhalyk, O. O.; Dunbar, A. D. F.; Hopkinson, P. E.; Donald, A. M.; Jones, R. A. L. *Macromolecules*

2011, 44, 6503–6508. See also: Ophir, Z.; Wilkes, G. L. *J. Polym. Sci., Polym. Phys.* **1980**, 18, 1469–1480.